

Thermal Equilibrium as an Initial State for Quantum Computation by NMR

Amr F. Fahmy,¹ Raimund Marx*,² Wolfgang Bermel,³ and Steffen J. Glaser†²

¹*Biological Chemistry and Molecular Pharmacology,*

Harvard Medical School, 240 Longwood Avenue, Boston, MA 02115, USA

²*Department of Chemistry, Technische Universität München, Lichtenbergstr. 4, D-85747 Garching, Germany*

³*Bruker Analytik GmbH, Silberstreifen, D-76287 Rheinstetten, Germany*

We present a method of using a nuclear magnetic resonance computer to solve the Deutsch-Jozsa problem in which: (1) the number of molecules in the NMR sample is irrelevant to the number of qubits available to an NMR quantum computer, and (2) the initial state is chosen to be the state of thermal equilibrium, thereby avoiding the preparation of pseudopure states and the resulting exponential loss of signal as the number of qubits increases. The algorithm is described along with its experimental implementation using four active qubits. As expected, measured spectra demonstrate a clear distinction between constant and balanced functions.

INTRODUCTION

Liquid state nuclear magnetic resonance (NMR) [1] has been used to demonstrate basic concepts of quantum information processing, including the realization of known quantum algorithms on a small number of qubits [2-7]. NMR has been leading the field both in terms of number of qubits and in terms of coherent control techniques. Never-the-less, liquid state NMR quantum computing is widely considered to be a futile effort because the preparation of certain initial states destroys an exponential amount of signal [8] and because it is not clear how to extract useful information by measuring expectation values.

Here, we present concepts that make it possible to directly use the high-temperature thermal equilibrium density operator as an initial state for quantum computing. We also show how to unitarily evolve this thermal state into a state from which useful information can be extracted. Clearly, a key ingredient of quantum information processing is the availability of an accessible (and controllable) state space that grows exponentially with the number of qubits and the ability to create superpositions of these states. This requirement applies both to pure and mixed state quantum computing. In the case of pure states, the set of all superpositions necessarily includes entangled states. However, in mixed state quantum ensembles, the ability to create (coherent) superpositions of an exponentially increasing number of states does not necessarily imply that the density operator describing the ensemble must be non-separable [9] at each point in time. In fact, we argue that the concept of sep-

arability is of little relevance (if any) for the question whether a given experimental implementation of a quantum algorithm is quantum or not. Furthermore, it is important to note that for ensemble quantum computing algorithms which are based on coherent superpositions of basis states, the accessible exponential state space is not limited by the number of molecules in the sample.

Here, we discuss a version of the Deutsch-Jozsa algorithm [10-12] for an NMR quantum computer that does not try to directly mimic a pure state algorithm. This demonstrates that a new set of algorithms is needed for this kind of computer. So far, there has not been an easy way to describe algorithms or unitary evolution on the density matrix of mixed states that is meaningful from the quantum computing point of view. Here we introduce the concept of acting on outer products, where the use of an extra control spin allows us to act only on one side of the outer product. This allows us to preserve and use phase information. We show that the signal-to-noise ratio of the presented algorithm does not diminish as the number of spins per molecule is increased, provided the total number of molecules in the ensemble is constant. We show that this approach provides an accessible state space that is of exponential size in the number of spins per molecule. In addition to the theoretical discussion, we present the first experimental implementation of this version of the Deutsch-Jozsa algorithm that does not suffer from the scaling problems associated with the preparation of pseudopure states [8].

COMPUTATION ON ONE VS MANY MOLECULES

By "molecule" we mean an isolated quantum system. In the first subsection we address computation on one molecule that is restricted to be in basis states, this will

*Raimund Marx and Amr F. Fahmy both equally contributed to this article

†to whom correspondence should be addressed: glaser@ch.tum.de

correspond to classical computation. Next, we address computation still on a single molecule that is allowed to be in superposition states of the chosen basis states, this will correspond to pure state quantum computation. After this, we will talk about computation on many molecules in the two cases covered for the single molecule case. We will see that NMR is capable of quantum parallelism over an exponential state space that is allowed to be in coherent superposition.

Computation on a single molecule

Computation on a single molecule restricted to basis states

In this case we have a state function that starts in some basis state (from the exponential number of computational basis states) say state $|0\rangle$. A computation consists of logical gates which correspond to transitions from the initial basis state to some other basis state

$$|\psi\rangle = |j\rangle, \quad 0 \leq j \leq N-1$$

via permutations only, where N is the size of the Hilbert space. The spins are never allowed to be in a superposition state. The initial density matrix $|\psi\rangle\langle\psi| = |j\rangle\langle j|$ for this system is a diagonal matrix with a single non-zero entry. During the computation, the single non-zero entry is permuted from one place to another on the diagonal. This corresponds to classical computation and is not more powerful than a classical computer even though a quantum system is used.

Computation on one molecule in superposition of basis states

Here we have a system that is allowed to be in superposition of the form

$$|\psi\rangle = \sum_{j=0}^{N-1} c_j |j\rangle.$$

Acting with a quantum gate (general unitary transformation) on a superposition is referred to as quantum parallelism where, in general, an exponential number of computational threads take place in parallel. The density matrix of this system is of the form $|\psi\rangle\langle\psi|$ where non-diagonal elements are non-zero in the presence of superpositions of the basis states. The control and manipulation of superpositions is a key ingredient that makes quantum computers more powerful than classical computers. This type of computation is referred to as pure state quantum computing in the literature [13].

Computation on many molecules

In this subsection we turn to computation using many copies of the same molecule. The density matrix for each case is simply defined as the average of the density matrices of the individual molecules in the ensemble.

Computation on diagonal density matrices

Here we consider the case where the initial state of each molecule in the ensemble is a basis state. If the initial state of each molecule happens to be the same then we have multiple copies of the case discussed above and the ensemble behaves in exactly the same way. In general however, each molecule may be in a different initial basis state and the density matrix of the ensemble is diagonal and may have more than one non-zero diagonal entry. Consider an example with two molecules with one spin each with the following state functions

$$|\psi^{(1)}\rangle = |0\rangle, \quad \text{with } |\psi^{(1)}\rangle\langle\psi^{(1)}| = \begin{pmatrix} 1 & 0 \\ 0 & 0 \end{pmatrix},$$

$$|\psi^{(2)}\rangle = |1\rangle, \quad \text{with } |\psi^{(2)}\rangle\langle\psi^{(2)}| = \begin{pmatrix} 0 & 0 \\ 0 & 1 \end{pmatrix}.$$

The corresponding density operator is

$$\rho = 1/2 \begin{pmatrix} 1 & 0 \\ 0 & 1 \end{pmatrix}.$$

If the ensemble is operated upon by permutations which keep the density matrix diagonal, this will correspond to parallel classical computation, where each molecule may be considered as a separate classical computer [14, 15].

Note that the number of molecules is very important in this case since this is where the parallelism is coming from. If each molecule contains n spins, the dimension of the density matrix is $2^n \times 2^n$ and in order for the diagonal of the density matrix to be fully occupied, at least 2^n molecules will be required [15].

The same conclusion holds for any ensemble that is described by a diagonal density operator throughout the computation. A diagonal density operator does not require that all molecules are in basis states, as off-diagonal matrix elements can average to zero. For example, for two states given by:

$$|\psi^{(1)}\rangle = \frac{1}{\sqrt{2}}(|0\rangle + |1\rangle), \quad \text{with } |\psi^{(1)}\rangle\langle\psi^{(1)}| = \frac{1}{2} \begin{pmatrix} 1 & 1 \\ 1 & 1 \end{pmatrix},$$

$$|\psi^{(2)}\rangle = \frac{1}{\sqrt{2}}(|0\rangle - |1\rangle), \quad \text{with } |\psi^{(2)}\rangle\langle\psi^{(2)}| = \frac{1}{2} \begin{pmatrix} 1 & -1 \\ -1 & 1 \end{pmatrix},$$

the density operator is also given by

$$\rho = 1/2 \begin{pmatrix} 1 & 0 \\ 0 & 1 \end{pmatrix}.$$

Computation on off diagonal density operators

Off-diagonal elements of the density operator can only occur if a subpopulation of the molecules exists whose state functions are superpositions of the computational basis states. For example, in an ensemble of two molecules containing one spin each, the density operator

$$\rho = \frac{1}{2} \begin{pmatrix} 1 & 1 \\ 1 & 1 \end{pmatrix}$$

requires that for each molecule, the state function has the form $|\psi^{(k)}\rangle = \frac{1}{\sqrt{2}}e^{i\theta_k}(|0\rangle + |1\rangle)$ with arbitrary phase factors $e^{i\theta_k}$ for $k = 1, 2$.

We note that an ensemble of M identical molecules where each molecule contains n spins has a density operator that is the same size as the density operator of a single molecule and behaves in the same manner under application of unitary transforms. If it is possible to prepare a density operator with off diagonal elements and manipulate these terms, one will have a computer as powerful as a pure state quantum computer except for the measurement step which we shall address below. In contrast to the previous example, we note that what is important for the size of the available state space is the number of spins per molecule and not the number of molecules in the ensemble.

ENSEMBLES OF ISOLATED QUANTUM SYSTEMS

In NMR implementations, the ensemble consists of M identical molecules. In every molecule, the nuclear spins form an isolated quantum system. Here, we assume that each molecule contains $n + 1$ spins. (In the following sections, we will explain why we chose $n + 1$ rather than n spins per molecule). The resonance frequency of each spin is $\omega_l = -\gamma_l B_0$ where γ_l is the gyromagnetic ratio of spin l and B_0 is the strength of the magnetic field. The state of the spin system corresponding to molecule k is given by a wave function

$$|\psi^{(k)}\rangle = \sum_{j=0}^{N-1} c_j^{(k)} |j\rangle \quad (1)$$

where $|j\rangle$ are the standard basis states used in quantum computing, $c_j^{(k)}$ are the corresponding amplitudes and $N = 2^{n+1}$. The density operator of the ensemble is given by

$$\rho = \frac{1}{M} \sum_{k=1}^M |\psi^{(k)}\rangle \langle \psi^{(k)}|.$$

Each matrix element of the density operator is given by

$$\rho_{rs} = \frac{1}{M} \sum_{k=1}^M c_r^{(k)} c_s^{*(k)}. \quad (2)$$

The diagonal entries of the density matrix, i.e. when $r = s$, represent populations of the quantum basis states [1]. Non-zero off-diagonal elements of the density matrix represent *coherent* superpositions of states.

If all the state functions $|\psi^{(k)}\rangle$ are basis states, i.e. the quantum system k is not in a superposition of the basis states, the product $c_r^{(k)} c_s^{*(k)}$ must be zero. Hence a necessary (albeit not sufficient) condition for an off-diagonal element ρ_{rs} to be non-zero is that molecules exist whose individual quantum systems are in a superposition of the basis states $|r\rangle$ and $|s\rangle$, i.e. for each of these molecules the state $|\psi^{(k)}\rangle$ is of the form given in equation (2) with $c_r^{(k)} \neq 0$ and $c_s^{(k)} \neq 0$. The ensemble is said to contain coherence [1] between the basis states $|r\rangle$ and $|s\rangle$ if the sum of the terms $c_r^{(k)} c_s^{*(k)}$ over all molecules is non-zero, c.f. (2). This implies that the available state space is exponential in the number of spins per molecule. One can compute with the diagonal elements only [14], however even in the best case when each molecule is in a different basis state, the size of the state space available for computation is bounded by the number of molecules in the sample [15]. Indeed in this case we simply have computation by classical parallelism. This contrasts to computing with off-diagonal elements [16] as we shall see in the following.

THERMAL EQUILIBRIUM

The thermal equilibrium of an ensemble of spin systems is described by the Boltzmann distribution where the probability of the system being in state $|r\rangle$ is given by

$$p(|r\rangle) = \frac{\exp(-E_r/kT)}{\sum_{j=0}^{N-1} \exp(-E_j/kT)},$$

where E_r is the energy of the r^{th} eigen state of the Hamiltonian of the system, k is Boltzmann's constant and T is temperature.

If we assume that there are no coherences at thermal equilibrium [1] the density operator of the system can be written as [1]

$$\rho_{th} \approx \frac{\exp(-H/kT)}{\text{Tr}(\exp(-H/kT))} \approx \frac{1}{N} \left(\mathbf{1} - \frac{H}{kT} \right)$$

for $\|H\| \ll kT$.

In a system where the size of the couplings between the spins is much less than the resonance frequencies ω_l of the individual spins I_l , the thermal density operator can be approximated by [1]

$$\rho_{th} \approx \frac{1}{N} \left(\mathbf{1} - \sum_{l=1}^{n+1} \alpha_l I_{lz} \right) \quad (3)$$

with $\alpha_l = \frac{\hbar\omega_l}{kT}$ and

$$I_{lz} = \frac{1}{2} \mathbf{1} \otimes \dots \otimes \mathbf{1} \otimes \sigma_z \otimes \mathbf{1} \otimes \dots \otimes \mathbf{1},$$

where the Pauli matrix σ_z appears as the l^{th} term in the product.

UNITARY EVOLUTION, MEASUREMENT AND INITIAL STATE PREPARATION

All the topics of this section are standard in the NMR literature, see e.g. [1]. Application of a unitary transform U , whether by application of rf-pulses or by time evolution of the coupling Hamiltonian, to a density operator is obtained from

$$\rho' = U\rho U^\dagger.$$

The expectation value of a Hermitian operator A is

$$\langle A \rangle = \text{Tr}(A \rho).$$

For example, for the thermal density operator ρ_{th} , the expectation value of $F_z = \sum_{l=1}^{n+1} I_{lz}$ is

$$\begin{aligned} \langle F_z \rangle_{th} &= \text{Tr}(F_z \rho_{th}) \\ &= \frac{1}{N} \text{Tr}(F_z - F_z \sum_{l=1}^{n+1} \alpha_l I_{lz}) \\ &= -\frac{1}{4N} \sum_{l=1}^{n+1} \alpha_l \text{Tr}(\mathbf{1}) \\ &= -\frac{1}{4} \sum_{l=1}^{n+1} \alpha_l, \end{aligned}$$

where the facts that F_z is traceless, $\text{Tr}(\mathbf{1}) = N$ and $I_{lx}^2 = \frac{1}{4}\mathbf{1}$ were used. Note that as the number n of spins per molecule increases, so will the magnitude of the measured signal $\langle F_z \rangle_{th}$ for $\alpha_l > 0$. In contrast, for the density operator

$$\rho_0 = \frac{1}{N}(\mathbf{1} + \alpha_1 I_{1z}), \quad (4)$$

the expectation value of F_z is independent of n :

$$\langle F_z \rangle = \text{Tr}(F_z \rho_0) = \frac{\alpha_1}{4}, \quad (5)$$

which is identical to $\langle I_{1z} \rangle = \text{Tr}(I_{1z} \rho_0)$. (In NMR, ρ_0 can be created from ρ_{th} using standard procedures, e.g. by a combination of unitary transforms and pulsed field gradients.)

Application of the Hadamard transform (or of a 90_y° pulse) to ρ_0 results in the density operator

$$\rho_1 = \frac{1}{N}(\mathbf{1} + \alpha_1 I_{1x}), \quad (6)$$

for which the expectation value of F_x (and of I_{1x}) is also $\alpha_1/4$.

SCALING BEHAVIOR

As discussed in the previous section, for ρ_1 the expectation value $\langle I_{1x} \rangle$ is independent of the number of spins per molecule. Hence, the signal-to-noise ratio for a resolved resonance line of a molecule containing 3 spins is the same as for a molecule with 10^4 spins, assuming the same number of molecules is in the sample, i.e. if the molar concentration is the same.

As we saw earlier, there are no scaling problems with preparation of ρ_1 as an initial state for the computation starting from the thermal density operator ρ_{th} . Hence, a scalable mixed-state based quantum algorithm can be constructed if the following two conditions hold:

- (1) Use of ρ_1 as an initial state for the computation.
- (2) The decision about the problem being solved is based upon the expectation value of I_{1x} , where I_{1x} is either parallel or orthogonal to the traceless part of the final density operator.

An algorithm meeting these two conditions would overcome the arguments against scalability of NMR quantum computing [8]. (However, just as in pure state quantum computation, still a large number of practical or technological impediments for realization of large-scale quantum computers would remain, such as losses due to decoherence etc.) In the following section we will describe such an algorithm.

THE ALGORITHM

The starting state for the algorithm is formed by the density matrix ρ_1 (c.f. Eq. (6)), the traceless part of which is proportional to I_{1x} . As indicated in the previous sections, ρ_1 can be prepared from the thermal density operator ρ_{th} without any loss of signal as a function of the number of spins per molecule.

The key observation that allows us to use I_{1x} in the computation is that I_{1x} is the sum of all outer products which differ only in the state of the first spin:

$$I_{1x} = \frac{1}{2} \sum_{j=0}^{N'-1} |0, j\rangle\langle 1, j| + |1, j\rangle\langle 0, j|$$

where $N' = N/2$. Note that j runs from 0 to $N' - 1$, hence the size of the state space available for calculation is $N' = 2^n$ which is exponential in the number of spins per molecule and is independent of the number of molecules in the sample. We will exploit this structure and use it to apply unitary transforms to the outer products representing the states where spin 1 is in the state $|1\rangle$ only. Application of a unitary transform U (not controlled by spin 1) to I_{1x} results in a sum of outer products where the ket and the bra do not contain information that we can directly use for the Deutsch-Jozsa problem. Instead we consider the effect of using controlled unitary

operations cU . For a unitary transform U over n spins, it is not hard to construct the unitary transform cU over $n + 1$ spins which applies U to spins 2 to $n + 1$ if spin 1 is in state $|1\rangle$ and does nothing otherwise [17]. The control spin is unaffected in either case.

$$\begin{aligned} cU|1\rangle|j\rangle &= (\mathbf{1} \otimes U)|1\rangle|j\rangle = |1\rangle U|j\rangle \\ cU|0\rangle|j\rangle &= |0\rangle|j\rangle \end{aligned}$$

For the Deutsch-Jozsa problem, given the function f , which is promised to be either constant or balanced, we are given a unitary transform which acts as follows:

$$U_f|j\rangle = (-1)^{f(j)}|j\rangle.$$

It is desired to find out if f is balanced or constant by a single application of U_f .

The operator cU_f can be used to distinguish if f is a balanced or constant function using ρ_1 as the starting state. There are two steps to the algorithm:

1. Apply cU_f to ρ_1 to obtain the density operator $\rho_2 = \frac{1}{N}(\mathbf{1} + \alpha_1 cU_f I_{1x} cU_f^\dagger)$.
2. Measure I_{1x} , i.e. find the value of $Tr(I_{1x}\rho_2)$. A value of $\alpha_1/4$ will indicate that f is constant and 0, a value of $-\alpha_1/4$ will indicate that the function is constant and 1, and a value of 0 indicates that f is a balanced function as we shall see next.

For the first step, apply cU_f to ρ_1 to get

$$\begin{aligned} \rho_2 &= \frac{1}{N}(\mathbf{1} + \alpha_1 cU_f I_{1x} cU_f^\dagger) \\ &= \frac{1}{N}(\mathbf{1} + \frac{\alpha_1}{2} \sum_{j=0}^{N'-1} \{cU_f|0, j\rangle\langle 1, j|cU_f^\dagger + \\ &\quad cU_f|1, j\rangle\langle 0, j|cU_f^\dagger\}) \\ &= \frac{1}{N}(\mathbf{1} + \frac{\alpha_1}{2} \sum_{j=0}^{N'-1} \{|0, j\rangle\langle 1, j|(\mathbf{1}_2 \otimes U_f^\dagger) + \\ &\quad (\mathbf{1}_2 \otimes U_f)|1, j\rangle\langle 0, j|\}) \\ &= \frac{1}{N}(\mathbf{1} + \frac{\alpha_1}{2} \sum_{j=0}^{N'-1} \{(-1)^{f(j)}|0, j\rangle\langle 1, j| + \\ &\quad (-1)^{f(j)}|1, j\rangle\langle 0, j|\}). \end{aligned}$$

The second step is the measurement of I_{1x} which produces

$$\begin{aligned} Tr(\rho_2 I_{1x}) &= \frac{\alpha_1}{4N} \sum_{j=0}^{N'-1} \{(-1)^{f(j)} + (-1)^{f(j)}\} \\ &= \begin{cases} \frac{\alpha_1}{4} & \text{if } f \text{ is constant and } 0 \\ -\frac{\alpha_1}{4} & \text{if } f \text{ is constant and } 1 \\ 0 & \text{if } f \text{ is balanced.} \end{cases} \end{aligned}$$

As in the pure state case, the measurement produces the same answer every time it is performed. Thus, the algorithm is deterministic.

EXPERIMENTS

Here, an experimental demonstration of the algorithm is presented. The experiments are based on the spin system of BOC-($^{13}\text{C}_2$ - ^{15}N - $^2\text{D}_2^\alpha$ -glycine)-fluoride [18] which forms a five-qubit system. In the present application, only four of the five qubits were used explicitly in the implemented algorithm (although it was necessary to eliminate interactions of the fifth qubit with the qubits that play an active role in our experiments). For convenience, here we will use the following labels for the qubits: the nuclear spins of the carbonyl $^{13}\text{C}'$, the aliphatic $^{13}\text{C}^\alpha$, the ^{19}F , the ^{15}N and the amide ^1H atoms are labeled 1, 2, 3, 4, and 5, respectively.

For our demonstration experiments, we chose the following test functions on $n = 3$ qubits: The constant test function was

$$f_0(x_2, x_3, x_4) = 0 \quad (7)$$

and the balanced test function was

$$f_b(x_2, x_3, x_4) = x_2 x_3 \oplus x_4. \quad (8)$$

For convenience, from now on we will drop the identity operator from the description of the density matrix and set $\alpha_1 = 1$. Starting from thermal equilibrium, the (reduced) density operator $\rho_0 = I_{1z}$ is prepared by a sequence of INEPT-type transfers and pulsed field gradients starting from ^1H magnetization (proportional to I_{5z}) as explained in Ref. [18]. Application of a 90_y° pulse to ρ_0 yields the desired initial state $\rho_1 = I_{1x}$.

Practical pulse sequences that implement the unitary transformation cU_f corresponding to a given function can be derived from an effective Hamiltonian [1]

$$\mathcal{H}^{eff} = \frac{i}{\tau} \log cU_f \quad (9)$$

which effects the desired transformation in time τ . Note that there is an infinite number of solutions to Eq. (9) from which a convenient effective Hamiltonian \mathcal{H}^{eff} can be chosen that is compatible with the coupling topology of the available spin system [1]. For the balanced test function f_b defined in Eq. (8), cU_{f_b} is a diagonal unitary matrix in the standard computational basis and its diagonal elements are $\{1, 1, 1, 1, 1, 1, 1, 1, -1, 1, -1, 1, -1, -1, 1\}$. A convenient effective Hamiltonian corresponding to cU_{f_b} is

$$\begin{aligned} \mathcal{H}_b^{eff} &= \frac{\pi}{4\tau} \left\{ \frac{3}{2} \mathbf{1} - 3I_{1z} - I_{2z} - I_{3z} - 2I_{4z} + 2I_{1z}I_{2z} + \right. \\ &\quad \left. 2I_{1z}I_{3z} + 2I_{2z}I_{3z} + 4I_{1z}I_{4z} - 4I_{1z}I_{2z}I_{3z} \right\}. \end{aligned}$$

All product operator terms in \mathcal{H}_b^{eff} mutually commute and hence can be implemented independently and in arbitrary order. The term which is proportional to the

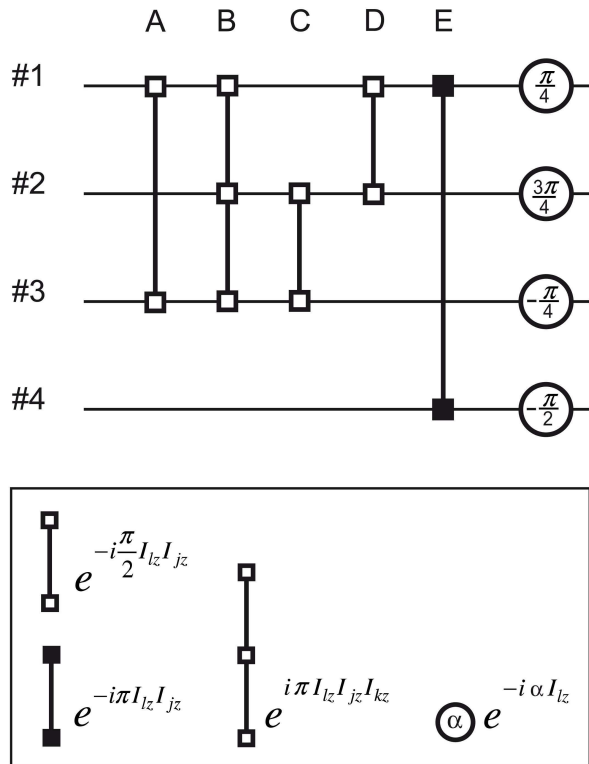


FIG. 1: Schematic representation of the decomposition of cU_{fb} given in Eq. (10). The symbols are defined in the inset. Up to local spin operations (see main text for details), the propagators A-E correspond to the pulse sequence elements A-E of the streamlined pulse sequence shown in Fig. 2.

identity operator can be neglected because it only contributes an irrelevant overall phase factor to the transformation cU_{fb} . A schematic representation of the transformations corresponding to this decomposition of U_{fb} is shown in Fig. 1.

The z rotations corresponding to the linear terms in H_b^{eff} can be implemented by composite pulses [19] or by phase shifts [18]. In the spin system of BOC-($^{13}\text{C}_2$ - ^{15}N - D_2^α -glycine)-fluoride, also the terms proportional to $I_{1z}I_{2z}$, $I_{1z}I_{3z}$, and $I_{2z}I_{3z}$ can be implemented in a straight-forward way, because the required couplings $J_{12} = 65.2$ Hz, $J_{13} = 366.0$ Hz, and $J_{23} = 67.7$ Hz [18] are non-zero and unwanted interactions can be removed by decoupling. However, qubit 1 and qubit 4 are not directly coupled, which requires the experimental simulation of the term proportional to $I_{1z}I_{4z}$. The present implementation of this bilinear term is based on the following transformation of the term $I_{2z}I_{4z}$ for which the experimental coupling constant is $J_{24} = 13.5$ Hz:

$$I_{1z}I_{4z} = V(I_{2z}I_{4z})V^{-1} \quad (10)$$

with

$$V = \exp\{-i\frac{\pi}{2}I_{1x}\}\exp\{-i\pi I_{1z}I_{2z}\}\exp\{-i\frac{\pi}{2}(I_{1y} + I_{2x})\}$$

$$\exp\{-i\pi I_{1z}I_{2z}\}\exp\{-i\frac{\pi}{2}I_{2y}\}.$$

Finally, the trilinear term in the effective Hamiltonian which is proportional to $I_{1z}I_{2z}I_{3z}$ was synthesized based on the transformation [20]

$$2I_{1z}I_{2z}I_{3z} = W(I_{1z}I_{2z})W^{-1} \quad (11)$$

with

$$W = \exp\{-i\frac{\pi}{2}I_{1x}\}\exp\{-i\pi I_{1z}I_{3z}\}\exp\{-i\frac{\pi}{2}I_{1y}\}. \quad (12)$$

The resulting pulse sequence elements can be simplified by standard procedures [18], e.g. by eliminating adjacent 180° pulses of the same phase or by transforming some pulses into z rotations that can be implemented by phase adjustments. For example, z rotations (by angle φ) can be implemented by a corresponding negative rotation of the respective rotating frame of reference. In practice, this results in an additional phase shift (by angle $-\varphi$) of all following r.f. pulses that are applied to this spin and of the receiver phase of this spin [18]. The theoretically derived pulse sequence elements for the individual terms in \mathcal{H}_b^{eff} were thoroughly tested experimentally on numerous initial density operator terms. A streamlined version of the pulse sequence implementing cU_{fb} is shown in Fig. 2.

The durations of the pulse sequences for each term in the effective Hamiltonian were chosen to be integer multiples of $\Delta = 1/|\nu_1 - \nu_2| = 81.75 \mu\text{s}$, in order to align the rotating frames of the homonuclear ^{13}C spins corresponding to qubits 1 and 2. The same pulse amplitudes and shapes were used for hard and selective pulses as in Ref. [18]. The bell-shaped symbols labeled “e” and “g” represent selective e-SNOB 90° pulses [21] (not for the usual 270° , but for a 90° rotation with a duration of $224 \mu\text{s}$) and selective Gaussian 180° pulses [22] (with a duration of $250 \mu\text{s}$ and a truncation level of 20%), respectively [18]. In order to avoid nonresonant effects of these selective ^{13}C pulses, a standard compensation scheme was used [23]. For example, during an e-SNOB 90° pulse applied to qubit 1 (offset 0 Hz), a second e-SNOB 90° pulse was applied at an offset frequency of -24.462 kHz, which cancels the nonresonant effects at the offset frequency of qubit 2 at the offset -12.231 kHz. During the selective e-SNOB 90° pulses, qubit 3 was actively decoupled by applying an MLEV-4 [24, 25, 26] expanded sequence of 180° pulses to spin 3 (boxes labeled “M”). During the entire experiment deuterium decoupling was applied using a WALTZ-16 sequence with $\nu_{rf} = 0.5$ kHz.

Segments A, B, C, D, and E are related to the bilinear or trilinear terms of the effective Hamiltonian \mathcal{H}_b^{eff} . Here, all propagators are implemented up to an overall (and irrelevant) phase factor. The propagator $\exp\{-i\frac{\pi}{2}I_{1z}I_{3z}\}$ is implemented by segment A and additional $(\pi)_{2x}$ and $(\pi)_{5x}$ rotations (shorthand notation for 180° rotations applied to qubits 2 and 5) at the end of the segment.

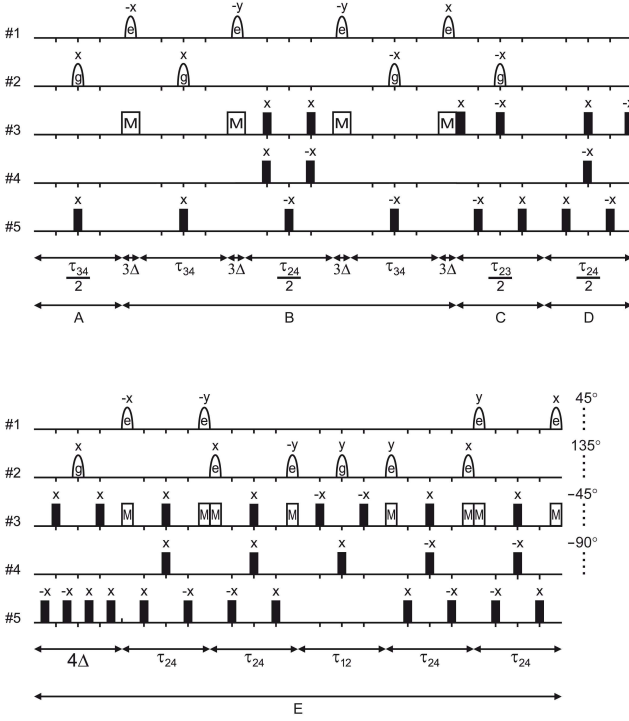


FIG. 2: Streamlined pulse sequence for the implementation of the unitary transformation cU_{f_b} . The durations $\tau_{kl} = 1/(2J_{kl})$ and $\tau_{kl}/2 = 1/(4J_{kl})$ were chosen to be integer multiples of $\Delta = 1/|\nu_1 - \nu_2| = 81.75 \mu\text{s}$ [18]. Filled rectangles represent 180° pulses. The bell-shaped symbols labeled “e” and “g” represent selective e-SNOB 90° pulses [21] and selective Gaussian 180° pulses [22], respectively. During the selective e-SNOB 90° pulses, qubit 3 was actively decoupled by applying an MLEV-4 [24, 25, 26] expanded sequence of 180° pulses to qubit 3 (boxes labeled “M”). Dotted vertical lines represent local z rotations. The overall duration of the pulse sequence is 84 ms.

The propagator $\exp\{i\pi I_{1z} I_{2z} I_{3z}\}$ is implemented by segment B and additional $(\pi)_{2x}$ and $(\pi)_{5x}$ rotations at the beginning of the segment and $(\pi)_{2x}$ and $(\pi)_{1z}$ rotations at the end of the segment. The propagator $\exp\{-i\frac{\pi}{2} I_{2z} I_{3z}\}$ is implemented by segment C and an additional $(\pi)_{2x}$ rotations at the beginning of the segment. The propagator $\exp\{-i\frac{\pi}{2} I_{1z} I_{2z}\}$ is implemented by segment D and an additional $(\pi)_{4x}$ rotations at the end of the segment. The propagator $\exp\{-i\pi I_{1z} I_{4z}\}$ is implemented by segment E and an additional $(\pi)_{4x}$ rotation at the beginning of the segment and a $(\pi)_{2z}$ rotations at the end of the segment. The additional $(\pi)_{2x}$ and $(\pi)_{5x}$ rotations at the end of segment A and at the beginning of segment B cancel and have been eliminated in the streamlined pulse sequence. Similarly, the remaining additional $(\pi)_{1x}$ and $(\pi)_{2x}$ rotations cancel. The additional $(\pi)_{1z}$ and $(\pi)_{2z}$ rotations commute with the remaining propagators and can be shifted to the end of the sequence, where they have been combined with the linear terms of $\mathcal{H}_b^{\text{eff}}$.

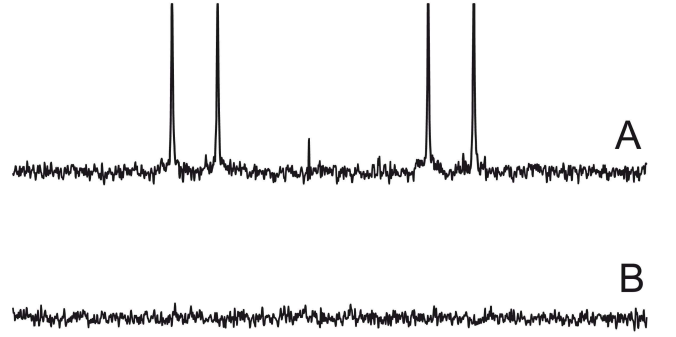


FIG. 3: Experimental results for (A) the constant function f_0 and (B) the balanced function f_b . The spectra show the signal of the carbonyl $^{13}\text{C}'$ spin of BOC- $(^{13}\text{C}_2\text{-}^{15}\text{N}\text{-}^2\text{D}_2^\alpha\text{-glycine})\text{-fluoride}$ [18] corresponding to qubit 1. Our NMR experiments were performed using a BRUKER AVANCE 400 spectrometer with five independent r.f. channels and a QXI probe (H,C-F,N). The lock coil was also used for deuterium decoupling utilizing a lock switch. The spectra with a spectral width of 900 Hz were acquired (128 scans) after applying the corresponding unitary transformations cU_{f_0} and cU_{f_b} to $\rho_1 = I_{1x}$.

Application of this pulse sequence to $\rho_1 = I_{1x}$ yields

$$\rho_1 = I_{1x} \xrightarrow{cU_{f_b}} \rho'_b = I_{1x} I_{4z} + 2I_{1x} I_{2z} I_{4z} + 2I_{1x} I_{3z} I_{4z} - 4I_{1x} I_{2z} I_{3z} I_{4z}.$$

None of the product operator terms in ρ'_b gives rise to detectable in-phase signal, i.e. the expectation value $\langle I_{1x} \rangle = \text{Tr}\{\rho'_b I_{1x}\}$ vanishes.

In general, a single time measurement of $\langle I_{1x} \rangle$ is sufficient to distinguish balanced from constant functions because $\langle I_{1x} \rangle$ is proportional to the integrated signal of the detected qubit in the frequency domain. If a full free induction decay (FID) is detected, it is possible to decouple all other qubits from the detected qubit 1, which makes the signal intensity of the detected spin (after Fourier transformation) independent of the number of coupled spins in the molecule. In our present demonstration experiments, decoupling was not used during the detection of the FID in order to show the details of the full multiplet structure of the signal of the detected qubit 1. In the special case of the coupling topology of BOC- $(^{13}\text{C}_2\text{-}^{15}\text{N}\text{-}^2\text{D}_2^\alpha\text{-glycine})\text{-fluoride}$, the operator ρ'_b cannot evolve into any observable signal under the free evolution operator because qubits 1 and 4 are not directly coupled. Hence, even if a full FID is acquired (rather than a single point measurement of $\langle I_{1x} \rangle$), no signal is expected. The experimental spectrum shown in Fig. 3B matches these theoretical predictions. For the balanced function, the spectrum in Fig. 3A shows four resolved inphase signals (a doublet of doublets due to the couplings J_{12} and J_{13}) with the expected intensity ratio of 1:1:1:1.

In order to demonstrate that the lack of signal in Fig. 3B is not simply due to artefacts or e.g. relaxation losses

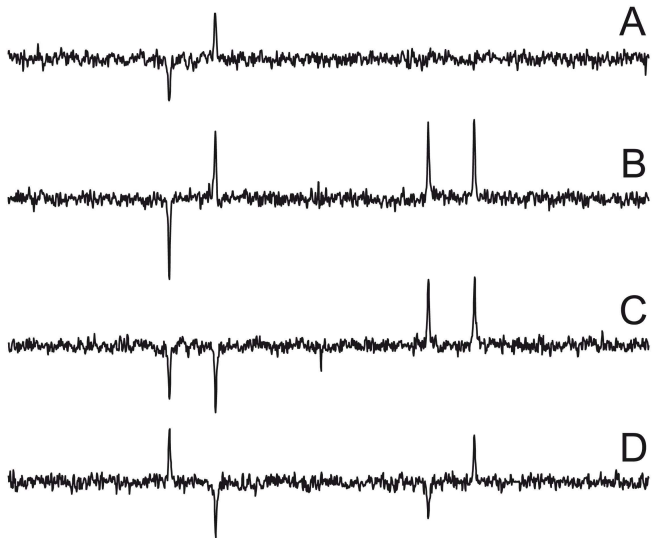


FIG. 4: Set of control spectra (128 scans) of qubit 1 after application of a $CNOT_{42}$ gate (with a duration of 37 ms) to ρ'_b (A) and application of the pulse sequence of cU_{f_b} (c.f. Fig. 2) to $2I_{1x}I_{4z}$ (B). The additional control spectra result if the pulse sequence corresponding to cU_{f_b} is applied to $\rho_0 = 2I_{1z}I_{3z}$ (C) and to $\rho_0 = 4I_{1z}I_{2z}I_{3z}$ (D), followed by a 90_y° read out pulse.

during the pulse sequence that implements cU_{f_b} (c.f. Fig. 2), we performed a series of control experiments. Application of the controlled-not operation $CNOT_{42}$ to ρ'_b yields

$$\rho'_b \xrightarrow{CNOT_{42}} \rho''_b = I_{1x}I_{4z} + \underline{I_{1x}I_{2z}} + 2I_{1x}I_{3z}I_{4z} - 2\underline{I_{1x}I_{2z}I_{3z}}, \quad (13)$$

where the underlined terms give rise to a doublet of doublet with an expected intensity ratio of $-1 : 1 : 0 : 0$. The corresponding experimental spectrum is shown in Fig. 4A.

If cU_{f_b} is applied to the initial density operator term $2I_{1x}I_{4z}$ (rather than to $\rho_1 = I_{1x}$), we find

$$2I_{1x}I_{4z} \xrightarrow{cU_{f_b}} \frac{1}{2} \underline{I_{1x}} + \underline{I_{1x}I_{2z}} + \underline{I_{1x}I_{3z}} - 2\underline{I_{1x}I_{2z}I_{3z}}, \quad (14)$$

where the underlined terms give rise to a doublet of doublet with an expected intensity ratio of $-1 : 1 : 1 : 1$. The corresponding experimental spectrum is shown in Fig. 4B. As \mathcal{H}_b^{eff} contains only longitudinal operators, it commutes with all density operator terms that contain only longitudinal operators. Hence, such density operator terms are invariant under the action of U_{f_b} . For example, for an initial density operator $2I_{1z}I_{3z}$ we expect

$$2I_{1z}I_{3z} \xrightarrow{cU_{f_b}} 2I_{1z}I_{3z} \xrightarrow{90_y^\circ(1)} \underline{2I_{1x}I_{3z}} \quad (15)$$

with an expected $-1 : -1 : 1 : 1$ multiplet (c.f. Fig. 4C)

and for an initial density operator $4I_{1z}I_{2z}I_{3z}$ we expect

$$4I_{1z}I_{2z}I_{3z} \xrightarrow{cU_{f_b}} 4I_{1z}I_{2z}I_{3z} \xrightarrow{90_y^\circ(1)} \underline{4I_{1x}I_{2z}I_{3z}} \quad (16)$$

with an expected $1 : -1 : -1 : 1$ multiplet (c.f. Fig. 4D). In all cases, a reasonable match is found between experimental results and theoretical predictions.

CONCLUSION

We introduced the concept of acting on outer products where the use of a control spin allows us to act only on one side of the outer product. This provides a lucid approach to construct and analyze a version of the Deutsch-Jozsa algorithm that is scalable in an NMR setting, where the quantum ensemble is initially at thermal equilibrium in the high temperature limit. The accessible state space is of exponential size in the number of spins per molecule and the available state space is not limited by the number of molecules in the ensemble. Most importantly, there is no exponential signal loss with the number of qubits.

The resulting algorithm has been implemented experimentally and a good match was found between theory and experiment. A crucial point in the implementation of the unitary transformation cU_{f_b} was the simulation of trilinear and bilinear coupling terms. The time-optimal simulation of bilinear [27] and trilinear [28] coupling terms can be used to further reduce the duration of pulse sequence elements used to implement the algorithm. The size of experimentally accessible liquid-state NMR quantum computers is not limited by fundamental scaling problems related to the preparation of an initial state, but by practical obstacles, such as the chemical synthesis of suitable molecules, the control of experimental imperfections and losses through decoherence and dissipation. However, similar questions are faced by all approaches to experimental quantum information processing. The fact that the Deutsch-Jozsa problem can be decided by a probabilistic classical algorithm should not be taken as a point against NMR. Since NMR technology can be used to decide on this problem deterministically by a single evaluation of the function, this should be an encouraging point to further study NMR and its capacity to solve other problems. It is an interesting open question if in general the thermal state can be used as an initial state for other algorithms and whether measuring expectation values of spin operators is useful for solving other problems.

ACKNOWLEDGMENTS

We thank J. Myers for numerous critical discussions. A. F. thanks Gerhard Wagner for support. S.J.G. thanks the integrated EU programme QAP, the DFG (Gl 203/4-2) and the Fonds der Chemischen Industrie for support.

-
- [1] R. R. Ernst, G. Bodenhausen, and A. Wokaun, *Principles of Nuclear Magnetic Resonance in One and Two Dimensions* (Oxford University Press, Oxford, 1987).
- [2] D. G. Cory, A. F. Fahmy, and T. F. Havel, *Proc. of the 4th Workshop on Physics and Computation* (New England Complex Systems Institute, Boston, MA, 1996), pp. 87–91.
- [3] D. G. Cory, A. F. Fahmy, and T. F. Havel, *Proc. Natl. Acad. Sci. USA* **94**, 1634 (1997).
- [4] N. A. Gershenfeld, and I. L. Chuang, *Science* **275**, 350 (1997).
- [5] J. A. Jones, *Phys. Chem. Comm.* **11**, 11 (2001).
- [6] S. Glaser, *Angew. Chem. Int. Ed.* **40**, 147 (2001).
- [7] C. Ramanathan, N. Boulant, Z. Chen, D. G. Cory, I. L. Chuang, M. Steffen, *Quant. Inf. Proc.* **3**, 15 (2004).
- [8] W. S. Warren, *Science* **277**, 1688 (1997).
- [9] S. L. Braunstein, C. M. Caves, R. Jozsa, N. Linden, S. Popescu and R. Schack, *Phys. Rev. Lett.* **83**, 1054 (1999).
- [10] D. Deutsch, and R. Jozsa, *Proc. Roy. Soc. London A* **439**, 553 (1992).
- [11] R. Cleve, A. Ekert, C. Macchiavello, and M. Mosca, *Proc. Roy. Soc. London A* **454**, 339 (1998).
- [12] D. Collins, K. W. Kim, and W. C. Holton, *Phys. Rev. A* **58**, R1633 (1998).
- [13] D. Deutsch, *Proc. R. Soc. Lond. A* **400**, 97 (1985).
- [14] M. Woodward, R. Brschweiler, *quant-ph/0006024* (2000).
- [15] Arvind, David Collins, *Phys. Rev. A* **68**, 052301 (2003).
- [16] J. M. Myers, A. F. Fahmy, S. J. Glaser and R. Marx, *Phys. Rev. A* **63**, 032302 (2001).
- [17] A. Barenco, C.H. Bennett, R. Cleve, D. DiVincenzo, N. Margolus, P. Shor, T. Sleator, J. Smolin, H. Weinfurter, *Phys. Rev. A* **52**, 3457 (1995).
- [18] R. Marx, A. F. Fahmy, J. M. Myers, W. Bermel and S. J. Glaser, *Phys. Rev. A* **62**, 012310 (2000).
- [19] R. Freeman, T. A. Frenkiel, and M. Levitt, *J. Magn. Reson.* **44**, 409 (1981).
- [20] C. H. Tseng, S. Somaroo, Y. Sharf, E. Knill, R. Laflamme, T. F. Havel, D. G. Cory, *Phys. Rev. A* **61**, 012302 (2000).
- [21] Ě. Kupĉe, J. Boyd, and I. D. Campbell, *J. Magn. Reson. B* **106**, 300 (1995).
- [22] C. Bauer, R. Freeman, T. Frenkiel, J. Keeler, and A. J. Shaka, *J. Magn. Reson.* **58**, 442 (1984).
- [23] M. A. McCoy, and L. Müller, *J. Magn. Reson.* **99**, 18 (1992).
- [24] M. H. Levitt, R. Freeman, and T. Frenkiel, *Adv. Magn. Res.* **11**, 47 (1983).
- [25] A. J. Shaka, J. Keeler, T. Frenkiel, and R. Freeman, *J. Magn. Reson.* **52**, 335 (1983).
- [26] U. Eggenberger, P. Schmidt, M. Sattler, S. J. Glaser, and C. Griesinger, *J. Magn. Reson.* **100**, 604 (1992).
- [27] N. Khaneja, B. Heitmann, A. Spörl, H. Yuan, T. Schulte-Herbrüggen, S. J. Glaser, *Phys. Rev. A* **75**, 012322 (2007).
- [28] N. Khaneja, S. J. Glaser, R. Bockett, *Phys. Rev. A* **65**, 032301 (2002).